Journal of Alloys and Compounds 509 (2011) 8413–8420

Contents lists available at ScienceDirect

Journal of Alloys and Compounds

journal homepage: www.elsevier.com/locate/jallcom

Novel hierarchical CdS crystals by an amino acid mediated hydrothermal process

Weiming Qiu[a,b], Mingsheng Xu[a,b,*], Xi Yang[a,b], Fei Chen[c], Yaxiong Nan[a,b], Hongzheng Chen[a,b,*]

[a] State Key Lab of Silicon Materials, Department of Polymer Science and Engineering, Zhejiang University, Hangzhou 310027, PR China
[b] Key Laboratory of Macromolecule Synthesis and Functionalization of Ministry of Education, Zhejiang University, Hangzhou 310027, PR China
[c] Laboratory of Polymer Materials and Engineering, Ningbo Institute of Technology, Zhejiang University, Ningbo 315100, PR China

ARTICLE INFO

Article history:
Received 1 March 2011
Received in revised form 24 May 2011
Accepted 28 May 2011
Available online 14 June 2011

Keywords:
Nanostructured materials
Hydrothermal crystal growth
CdS crystals
Amino acids

ABSTRACT

We report the synthesis of CdS crystals with novel dendritic structures by a simple amino acid mediated hydrothermal process, in which various amino acids were used as capping agents. We elaborated that a slight change of the side group of amino acids can significantly influence the type and the structure of CdS crystals. We found that the reaction temperature and the time also have effects on the formation of CdS crystals. The resulting different-shaped CdS crystals exhibited different UV–vis absorption characteristics. Our results suggest that the biomolecule-assisted hydrothermal route using amino acids as capping agents provides an effective and green approach to produce hierarchical CdS crystals with rich morphologies.

1. Introduction

Morphology-controlled synthesis of nano-/micro-crystals of semiconductor materials have attracted great interest because their optoelectronic properties are closely related to their sizes and shapes [1–8]. Compared to mono-morphological structures, hierarchical structures may show unique properties by combining the features of micrometer- and nanometer-scaled building blocks in one crystal [9–11]. Nano-/micro-sized CdS crystals show excellent optical and electronic properties and may have potential applications for solar cells, light-emitting diodes, hydrogen production, thin-film transistors, and photocatalysis [12–20]. Due to its unique properties and potential applications, considerable efforts have been made to develop effective approaches to synthesize CdS nano-/micro-crystals with different morphologies. Those methods include hydrothermal and solvothermal processes [21–24], chemical bath deposition [25], electrodeposition [26], vapor–liquid–solid assisted process [27], and colloidal method [28]. However, morphology-controlled fabrication of CdS nano-/micro-crystals with 3-dimensional (3D) structures *via* a solution-based process remains a major challenge due to the difficulty in controlling nucleation and growth [29,30], though hierarchically structured CdS crystals were reported [17,18,22,31–33].

Recently, biomolecule-assisted routes have been widely used in the preparation of various nanomaterials owing to the special structures and fascinating self-assembly functions of biomolecules. For instance, highly-ordered snowflake-like superstructures of Bi_2S_3 were prepared by using glutathione (GSH) as an assembling agent and as the sulfur source [34]. Cuprous oxide (Cu_2O) dendrites were prepared by using starch as a reducing and stabilizing agent [35]. Besides, CdS nanorod arrays [36] and other nanorod-based structures [33] have also been synthesized by biomolecule-assisted processes. Amino acids, as one of the most important categories of biomolecules, have attracted much attention in the past few years. For example, L-cysteine, which was widely used as a capping agent, has been used to fabricate ZnO nanorod arrays [37], In_2S_3 flower-like structures [38], PbS pagoda-like hierarchical architectures [39], NiS microcrystals [40], Sb_2S_3 microspheres [41], Ag_2S nanospheres [42], ZnS with complex 3D structure [43], and CdS nanospheres [17] by solution methods. However, there are few reports on synthesis of nanostructures by using other amino acids as structure-guiding agents in a hydrothermal process except L-cysteine, particularly in the synthesis of CdS crystals.

In this work, a wide variety of amino acids, such as L-valine, L-proline, L-serine, L-cysteine, L-methionine, L-histidine, and L-tryptophan, were exploited for the first time to synthesize CdS micro-/nano-crystals with various interesting morphologies by hydrothermal process. The types and the concentrations of amino acids as well as the reaction temperature and time were found to significantly influence the formation of CdS micro-/nano-crystals, which enable us to control the morphologies of CdS crystals.

* Corresponding authors at: State Key Lab of Silicon Materials, Department of Polymer Science and Engineering, Zhejiang University, Hangzhou 310027, PR China. Tel.: +86 571 87952557; fax: +86 571 87953733.
E-mail addresses: msxu@zju.edu.cn (M. Xu), hzchen@zju.edu.cn (H. Chen).

0925-8388/$ – see front matter © 2011 Elsevier B.V. All rights reserved.
doi:10.1016/j.jallcom.2011.05.103

2. Experimental

2.1. Synthesis of CdS nano-/micro-crystals

All chemicals used in this work were analytical grade, commercially available, and used without further purification. We used a traditional hydrothermal process to synthesize CdS crystals by changing the experimental parameters, such as different amino acids, reaction temperature, and reaction time. In a typical procedure, 1 mmol of $Cd(NO_3)_2$•$4H_2O$, 3 mmol of thiourea, and 0.3 mmol of L-valine were added into a given amount of distilled water and ultrasonicated for a few minutes. The resulting mixture was then transferred into a Teflon-lined stainless-autoclave (100 mL capacity), which was then sealed and maintained at 200 °C for 4 h. After that, the product was collected and washed with distilled water and ethanol several times, and then dried under vacuum for relevant characterizations. We used different kinds of amino acids, but kept other experiment unchanged unless specified, to investigate their effects on the synthesis of CdS crystals.

2.2. Characterization of CdS crystals

The phase of the as-prepared CdS products was determined by powder X-ray diffraction (XRD) using a Rigaku D/max-2550PC X-ray diffractometer with Cu-Kα radiation (λ = 1.5406 Å). The field emission scanning electron microscope (FE-SEM) images of CdS crystals were taken on a FESEM-4800 scanning electron microscope. Transmission electron microscope (TEM) images and the selected area electron diffraction (SAED) patterns were recorded on a JEM123 electron microscope and a JEOL-2010 high-resolution TEM at 200 kV. For TEM measurement, the product was ultrasonically dispersed in ethanol, and then the resulting suspension was dropped on a Cu grid coated with carbon film. Ultraviolet–visible (UV–vis) absorption spectrum of CdS crystals dispersed in ethanol was recorded on a PerkinElmer Lambda-35 spectrometer.

3. Results and discussion

All of the CdS samples synthesized here, regardless different conditions such as using different amino acids and varying reaction temperature and time, have a hexagonal structure as confirmed by the powder XRD measurement. For example, the diffraction peaks in Fig. 1 obtained from one of our CdS samples can be indexed to hexagonal CdS of wurtzite structure (JSPDS card No. 41-1049) with no obvious indication of impurities, except a small peak round 30.5° that may originate from the (0 0 2) peak of cubic phase CdS structures. The sharp and the strong peaks indicate that these CdS microstructures were highly crystallized. Furthermore, compared to the standard refraction, the intensity of (0 0 2) peak is much stronger, which indicates preferential orientation of our CdS crystals along the *c*-axis.

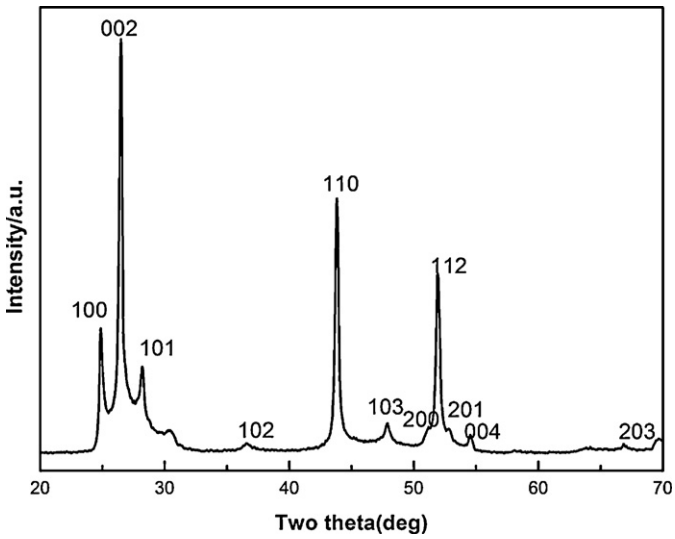

Fig. 1. XRD pattern for the product obtained by hydrothermal reaction of $Cd(NO_3)_2$ and thiourea with 0.3 mmol L-valine at 200 °C for 4 h.

To study the influence of amino acids on the formation and assembly of CdS crystals in the present hydrothermal synthesis, we selected a series of amino acids, whose chemical structures are illustrated in Scheme 1, as capping agents. Fig. 2 shows the typical SEM images of the CdS samples synthesized by using 0.3 mmol of L-valine, a very simple amino acid, as the capping agent and 1 mmol of $Cd(NO_3)_2$ and 3 mmol of thiourea as the Cd and S precursors, respectively, at 200 °C for 4 h. The low magnification image (Fig. 2(A)) shows that the CdS crystals have dendritic architectures with size up to several micrometers. It is revealed that each CdS dendrite is composed of one long main trunk (4–6 μm) and 6-fold symmetric rows of branches. The branches at the same longitude are separated by ~60° and the branches in a row are almost parallel with each other along the trunk (Fig. 2(B)–(D)).

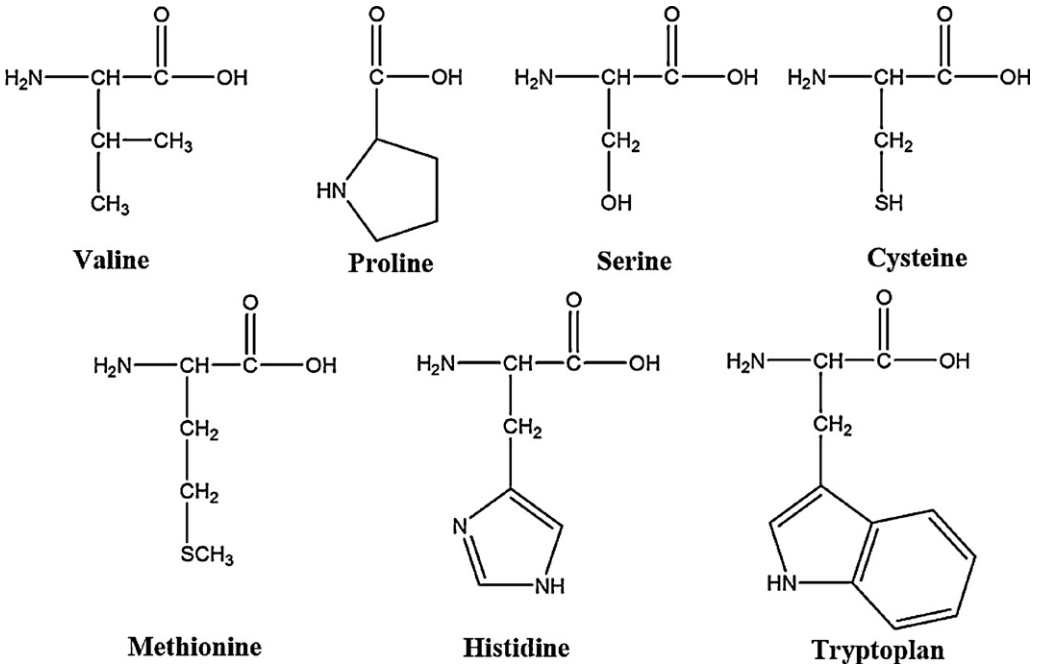

Scheme 1. Chemical structures of amino acids used in the present study.

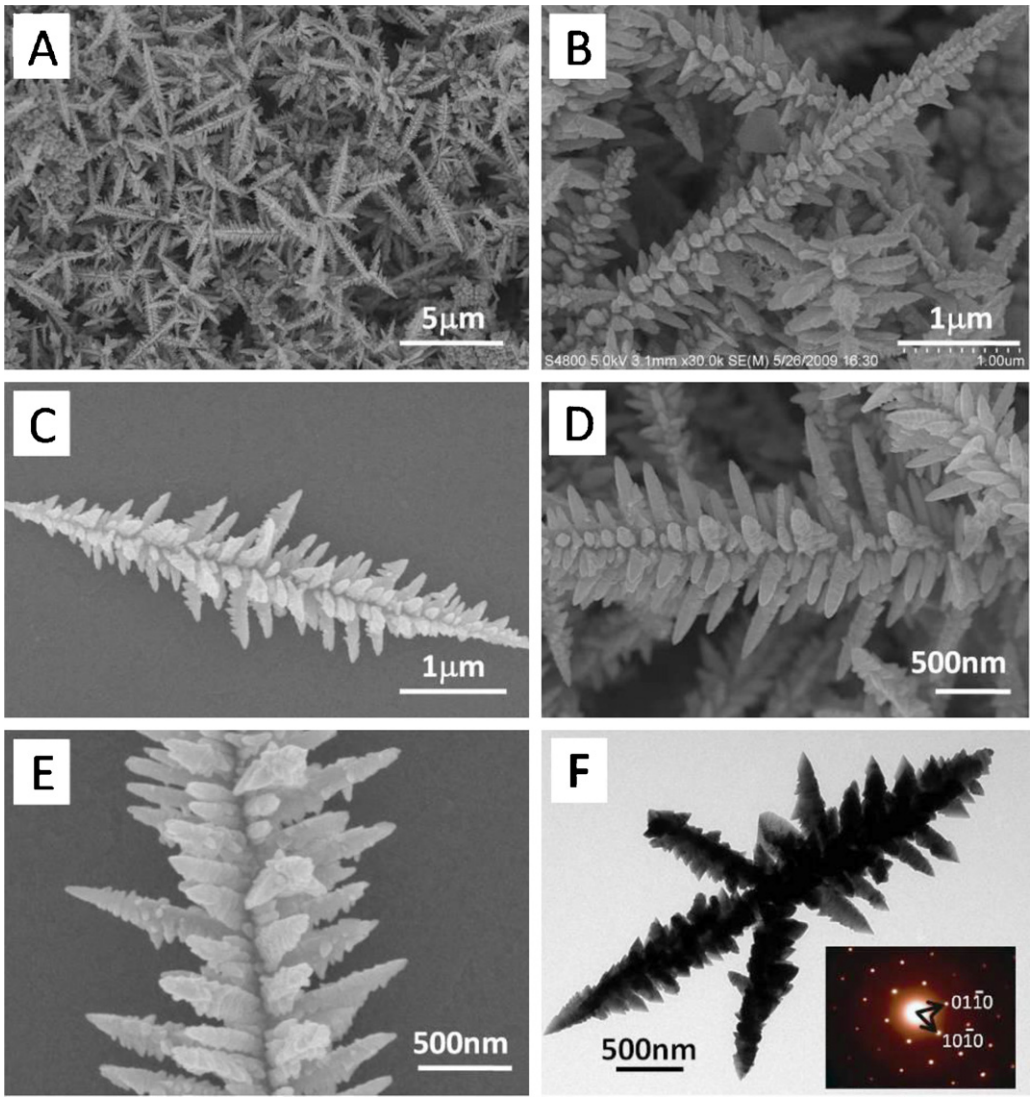

Fig. 2. SEM ((A)–(E)) and TEM (F) images of the CdS dendrites prepared with the assistance of L-valine at 200 °C for 4 h. The inset in (F) shows the SAED pattern corresponding to (0 0 0 1) planes.

The fine configuration of the dendrites is displayed in Fig. 2(E) and (F). Tertiary branches with the same symmetries as the main branches were formed on the main branches, suggesting that the whole architecture was resulted from the self-growth of the CdS nucleus rather than the accumulation of various crystals [22]. The selected area electron diffraction (SAED) pattern (Fig. 2(F)) collected from the main trunk tip and the branch tip is identical. These results suggest the CdS dendrites are finely crystallized wurtzite structures and the individual trunks and branches are single crystal.

Komarneni et al. [33,34] investigated the effects of type and structure of biomolecule, such as amino acids (glycine, serine), peptides (glycyl-glycine, glutathione), protein (gelatin, lysozyme), protein metabolism product (guanidine), RNA base (uracil), and pyrimidine (uridine), on the formation of CdS crystals, and found the morphology and structure of CdS crystals correspond to the used biomolecules' type and structure. Here we elaborate that although amino acids have similar structure which contains an $-NH_2$ group and a –COOH group, the subtle difference in the side group (–R) also greatly changes the formation and the structure of CdS products. Using L-proline which has a ring structure as the capping agent, we found that the regularity of the CdS products decreases remarkably (Fig. 3(B)), showing negligible difference from the CdS crystals synthesized without any additive (Fig. 3(A)). It may be attributed to the poor coordinating ability of L-proline stemming from the secondary amine and the hindrance from the ring structure, which in turn reduces the structure-directing function of L-proline. Furthermore, the existence of other functional groups on the side group may result in much more significant variations in the morphologies of CdS crystals. For example, by replacing L-valine with L-serine that has another –OH group in the present hydrothermal process, spindle-like CdS crystals with regularly arranged nanorods growing out of the main trunk (Fig. 3(C)) were synthesized. If L-cysteine was used as the capping agent, only CdS nanoparticles with 40–50 nm (Fig. 3(D)) were synthesized, without any CdS dendritic structure, which may be due to the strong reactivity between the –SH group and Cd^{2+}. However, by replacing the –SH of L-cysteine with $-SCH_3$, we produced a novel flower-like hierarchical pattern of CdS crystals using L-methionine as the capping agent (Fig. 3(E)). Fig. 3(F) displays the detailed characteristics of the petal of this novel architecture and the inset are the magnified pictures of the front and the back sides of the petal. These interesting results suggest that a slight change in the structure of the side group of amino acids can greatly change the coordinating habit of the amino acid for CdS growth and lead to novel morphologies of CdS crystals.

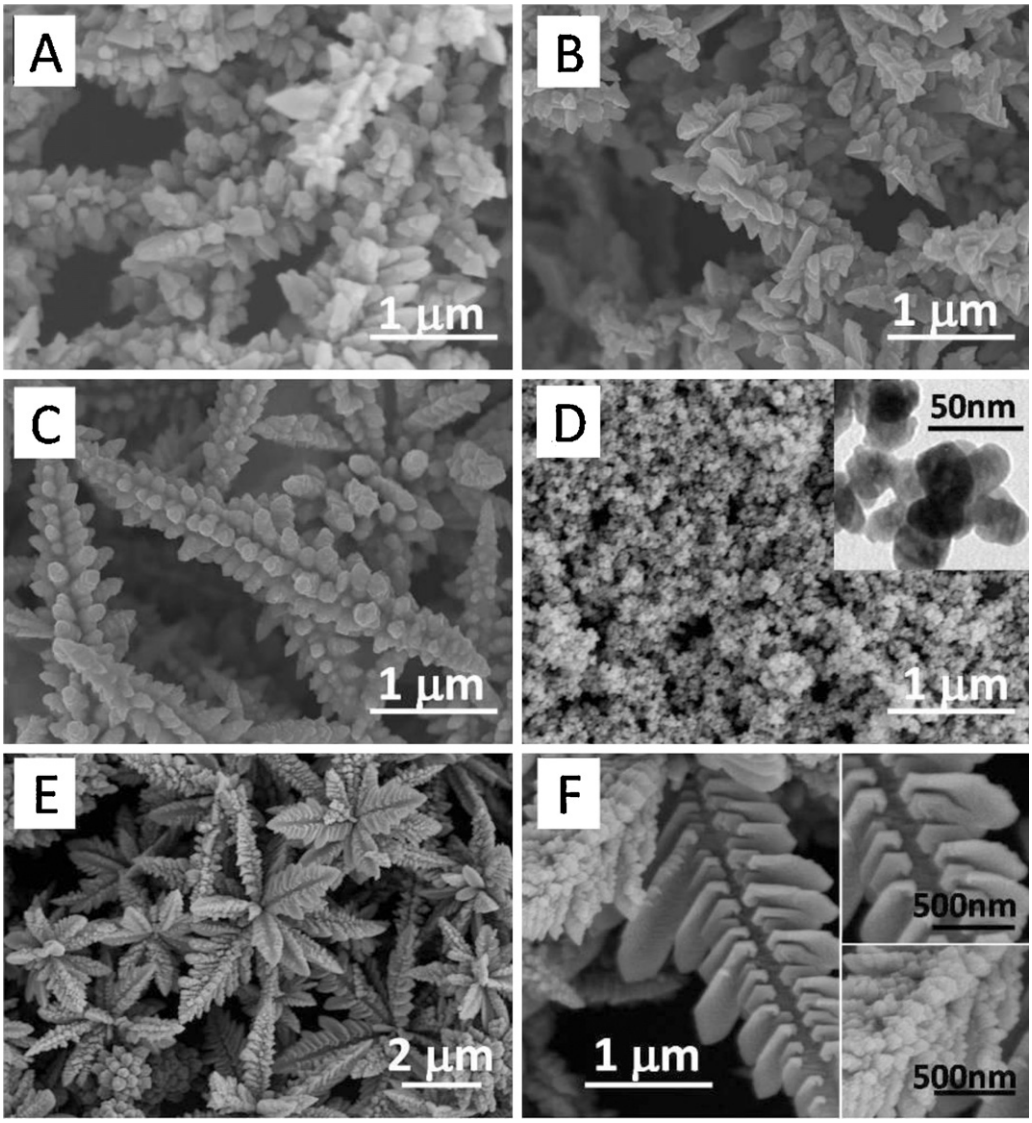

Fig. 3. SEM images of CdS crystals synthesized with different amino acids as capping agent at 200 °C for 4 h: (A) without amino acid, (B) L-proline, (C) L-serine, (D) L-cysteine, (E) and (F) L-methionine.

Inspired by the above morphological change, amino acids containing more complex side groups were further utilized as structure-directing additives to explore their capability to tailor the structure of CdS crystals. Fig. 4(A) and (B) shows the CdS crystals synthesized with the assistant of L-histidine. The CdS micropatterns have a radial architecture assembled by branch-like CdS crystals growing from the central part. Fig. 4(C) displays the as-prepared CdS crystals with L-tryptophan as the capping agent. The products consist homogeneously of CdS microcrystals with an interesting cauliflower-like architecture. It is revealed that this cauliflower-like structure is the self-assembly of thin leaf-like nanosheets. In addition, extending the reaction time from 4 h to 8 h produced a more complicated and delicate structure of CdS crystals as shown in Fig. 4(D).

We performed time-resolved investigation of the formation progress of dendritic CdS microcrystals with L-valine as the capping agent by quenching the reaction in Teflon-lined autoclave using cold water at different reaction time. When the reaction time was 1 h, the solution remained clear and transparent, and no precipitate was observed, indicating no CdS crystals were formed. Extending the reaction time to 2 h, CdS dendritic structures were formed, but the formed trunks and the branches were very short and with poor regularity (Fig. 5(A)). When the reaction time was increased to 4 h, very long and branched CdS dendrites with high regularity were obtained (Fig. 5(B)). However, if the reaction time was further extended to 8 h or even 12 h, it can be seen that the CdS crystals was overmatured and the regularity dramatically decreased, possibly due to the over-ripening of the nanostructures [19]. Based on these observations, we suggest that the CdS dendrites may form in a short period of time with a fast growth rate first and then undergo a ripping process which could destroy the regularity of the products if the ripping time was too long. Therefore, well-defined hierarchical dendrites with high regularity can be synthesized with an appropriate amino acid by controlling the reaction time.

Reaction temperature also has a fundamental effect on the shape of CdS crystals. Fig. 6(A)–(D) display the different morphologies of the CdS crystals synthesized by using L-valine as the capping agent at 160, 180, 200, and 220 °C, respectively. At 160 °C, only an urchin-like sphere structure was obtained (Fig. 6(A)). Extending the reaction time to 8 h (Fig. 6(E)) or even 12 h (Fig. 6(F)) at this temperature could not lead to well-defined CdS dendrites except irregularly structured products. At 180 °C, a mixture of dendrites with poor regularity and urchin-like spheres of CdS crys-

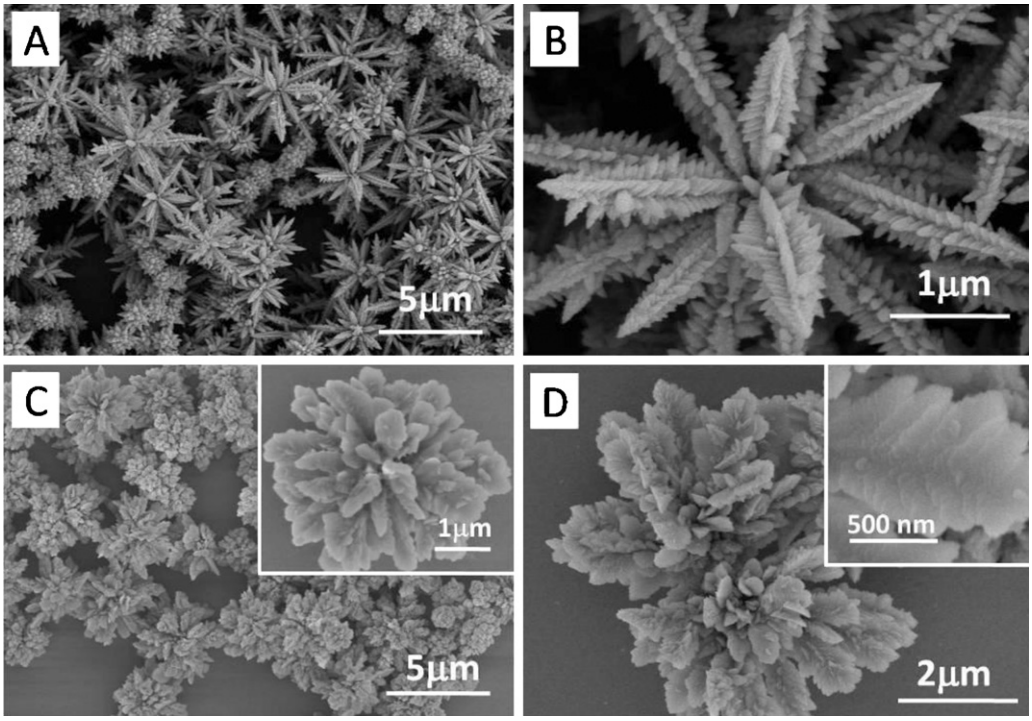

Fig. 4. SEM images of the CdS crystals prepared with the assistance of L-histidine (A) and (B) and L-tryptophan (C) and (D) at 200 °C, with a reaction time of 4 h for (A)–(C) and 8 h for (D). The insets of in (C) and (D) show a single urchin-like CdS crystal and the details of its typical leaf.

tals (Fig. 6(B)) were obtained. However, if the temperature was increased to 200 °C or higher to 220 °C, hierarchical CdS dendrites with high regularity and high yield were synthesized (Fig. 6(C) and (D)). These results suggest that CdS crystals with different shapes can be generated by control of reaction temperature.

Many studies have reported that the morphologies of nanocrystals are heavily dependent on the concentration of capping agents [18,21]. Here, we show that the amount of amino acid, for example L-valine, also greatly influences the morphologies of CdS crystals. With zero amount of L-valine, only irregular CdS crystals were

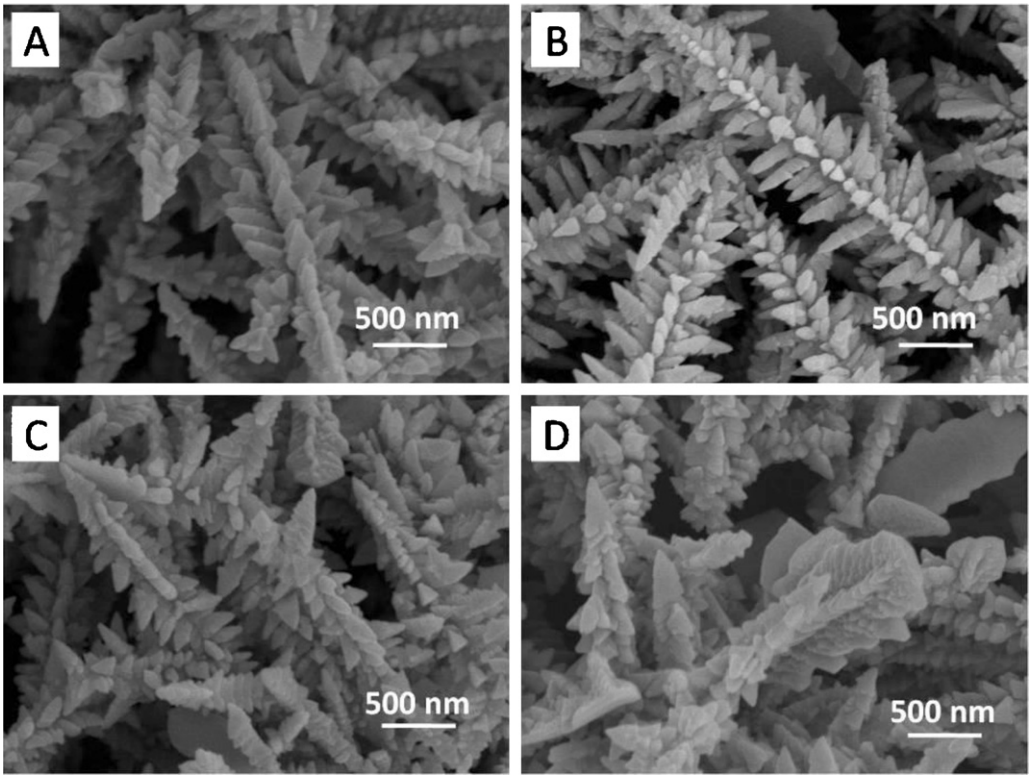

Fig. 5. Shape evolution of CdS crystals synthesized with 1 mmol $Cd(NO_3)_2$ and 3 mmol thiourea and 0.03 mmol L-valine at 200 °C as a function of reaction time: (A) 2 h; (B) 4 h; (C) 8 h and (D) 12 h.

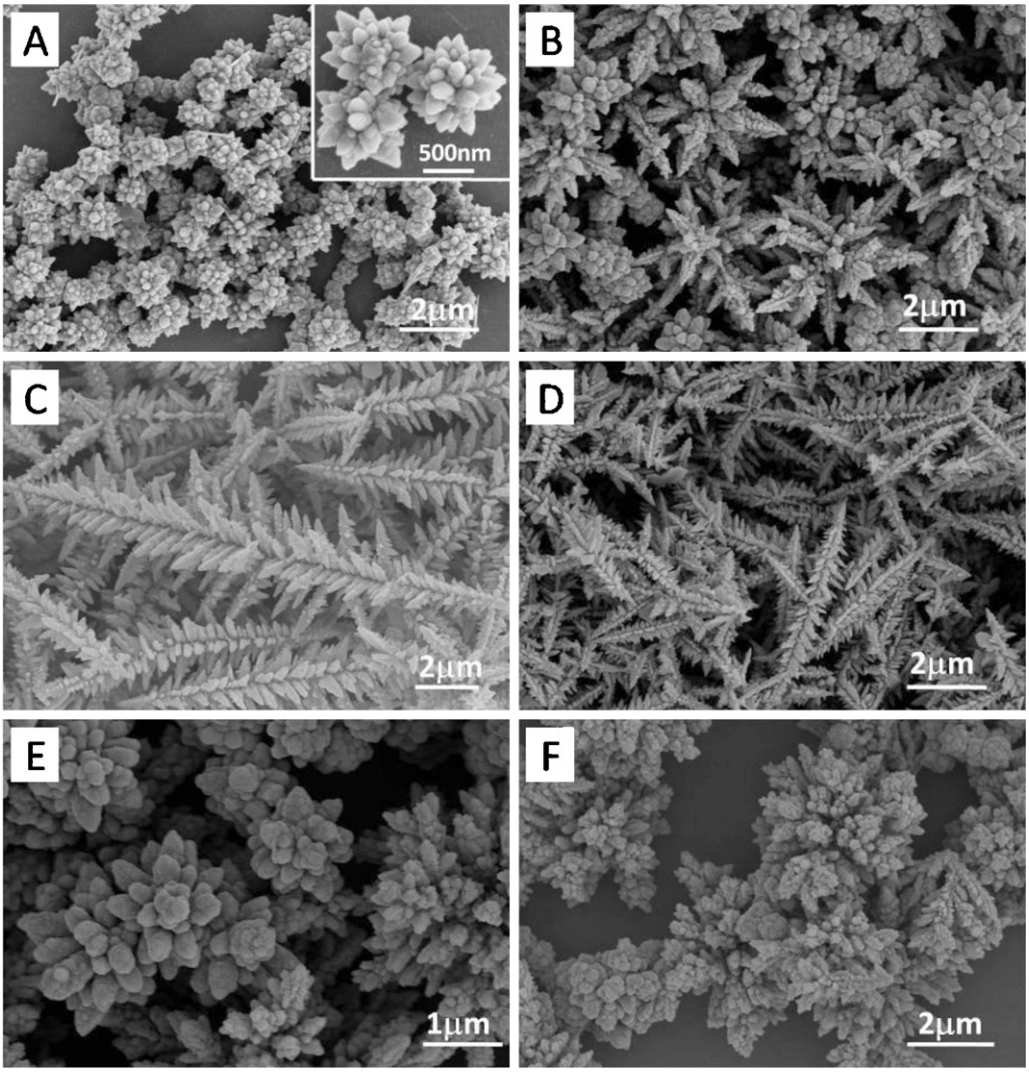

Fig. 6. SEM images of CdS crystals prepared at (A) 160 °C, (B) 180 °C, (C) 200 °C and (D) 220 °C for 4 h, (E) 160 °C for 8 h and (F) 160 °C for 12 h, with 1 mmol $Cd(NO_3)_2$ and 3 mmol thiourea and 0.03 mmol L-valine.

obtained (Fig. 7(A)). As the concentration of L-valine increased from 0.3 mmol to 0.9 mmol, and to 1.8 mmol, the morphology of CdS crystals was transformed from well-defined CdS dendrites (Fig. 7(B)) to leaf-like (Fig. 7(C)), and to novel flower-like (Fig. 7(D)) structures. The inset in Fig. 7(D) illustrates a single flower-like CdS crystal and the detailed petal. Furthermore, we also found that different amino acids show distinct functions in the morphological transformation of CdS crystals. In the case of using L-serine as the capping agent, the morphology of CdS crystals changed from spindle-like (Fig. 3(C)) to flower-like (Fig 7(E) and (F)) structures when the amount of L-serine increased from 0.3 mmol to 0.9 mmol, but the petals have more elaborate structures as compared to the CdS crystals obtained by using L-valine as the capping agent (Fig. 7(D)).

Although the exact growth mechanism of the above novel structured CdS crystals is not so clear, the hierarchical structures may form in a situation far from thermodynamic equilibrium [22,44,45]. Besides, soft template and selected absorption theory are used to explain the mechanism of crystal growth in the solution-based process where a capping agent is employed [23,46,47]. In the present synthesis, thiourea may act not only as the sulfur precursor, but also as a coordinate agent to form Cd^{2+}–thiourea complex, which might be a soft template for positioning a CdS nucleus to form dendrite structures [22,32]. At certain temperature and reaction time, thiourea is attacked by the strong nucleophilic O atoms of H_2O molecules, and this leads to weakening and breaking of the C=S double bonds to release the S^{2-} anion gradually. Consequently, the newly released S^{2-} reacts with Cd^{2+} to produce CdS nuclei. The gradual releasing of S^{2-} is a key process because it could ensure a stable monomer (Cd^{2+}–thiourea complex) concentration for anisotropic growth of CdS crystals. It had been pointed out that if Na_2S was used as the sulfur source, no dendrites could form with most of the S^{2-} consumed at the nucleation stage, due to the instantaneous releasing of S^{2-} [22,44]. Furthermore, during the growth, amino acid may selectively adsorb on certain facets of CdS seeds, resulting in the anisotropic growth of CdS crystals [33]. The ability of adsorption of amino acids on certain facets, *i.e.*, the coordinating behaviors of amino acids, is remarkably affected by their structures and concentrations, which can lead to the morphology of the dendrites different with each other. Particularly, for L-cysteine, it is easy to form the Cd^{2+}–L-cysteine complex which may also be readily to decompose to release S^{2-} and act as another sulfur source [17,39]. As a result, CdS crystals may grow in a different way and no hierarchical CdS structures can be synthesized (Fig. 3(D)).

The temperature-dependent morphology change indicates that the anisotropy growth of CdS crystals is favored at elevated reaction temperatures, in contrast to the formation of isotropic crystals such as urchin-like spherical CdS at relatively low reaction temper-

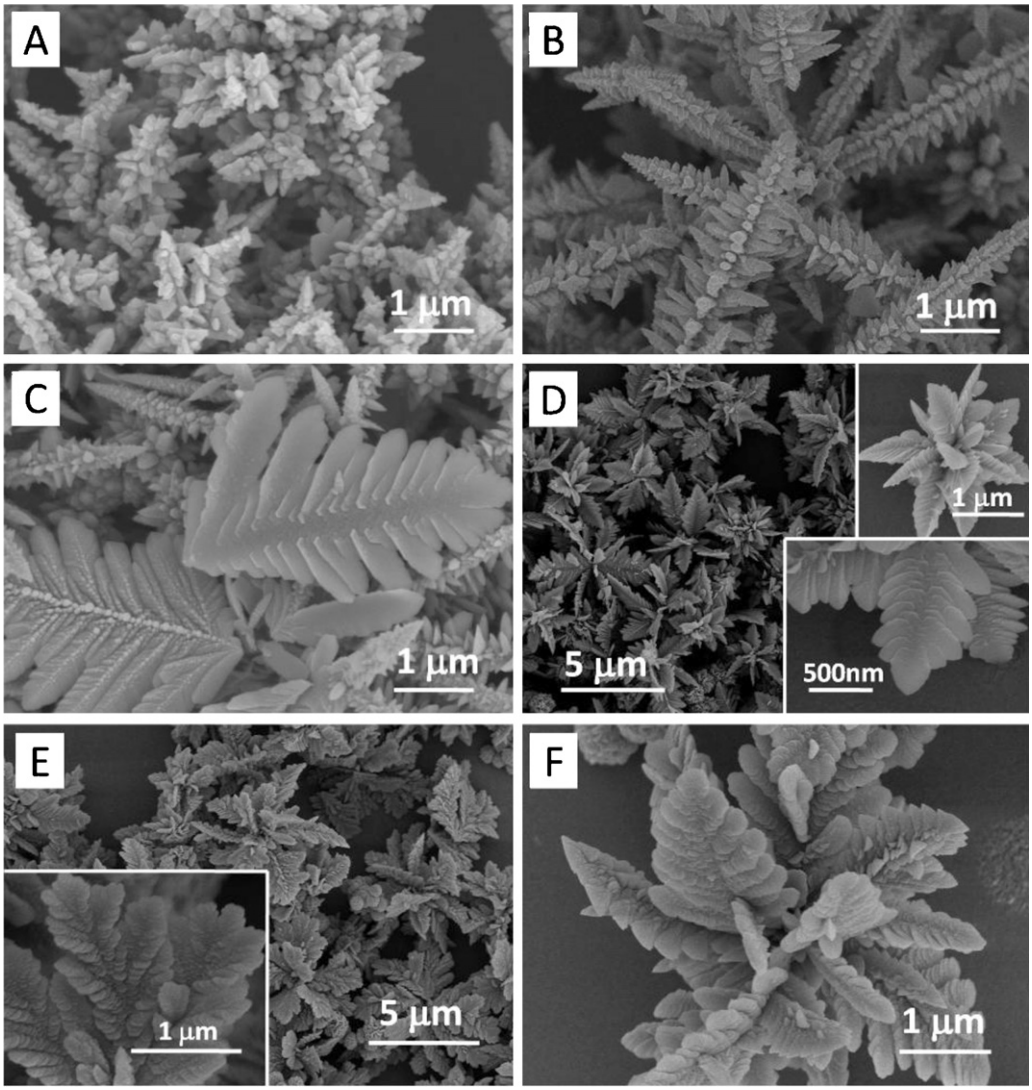

Fig. 7. SEM images of CdS crystals synthesized with 1 mmol $Cd(NO_3)_2$, 3 mmol thiourea and various amounts of amino acid at 200 °C for 4 h: (A) no L-valine, (B) 0.3 mmol L-valine, (C) 0.9 mmol L-valine, (D) 1.8 mmol L-valine, (E) and (F) 0.9 mmol of L-serine.

atures (Fig. 6(A)). The reason for temperature-dependent growth may lie in the fact that elevated reaction temperatures speed up the releasing of S^{2-} and accelerate the growth rate of CdS, and therefore the crystal growth is expected to be mainly under kinetic control rather than thermodynamic control, which consequently results in an anisotropic crystal morphology stemming from preferential growth along certain directions [21,48]. By contrast, the reduced releasing rate of S^{2-} at lower temperatures results in a slow growth rate and the thermodynamic control becomes dominant for CdS growth, leading to the formation of crystals with

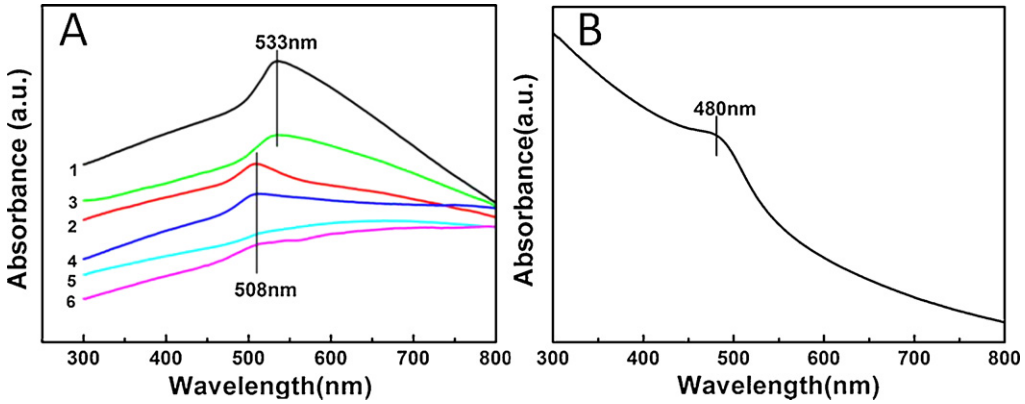

Fig. 8. UV–vis absorption spectra of various CdS crystals: (A) CdS dendrites shown in Fig. 2(A) (curve 1), Fig. 7(D) (curve 2), Fig. 3(C) (curve 3), Fig. 7(E) (curve 4), Fig. 3(E) (curve 5), and Fig. 4(C) (curve 6), (B) CdS nanoparticles shown in Fig. 3(D).

isotropic morphology [49,50]. This phenomenon is consistent with the observation of Alivisatos et al. [50], where formation of the nanocrystals with highly anisotropic shapes required a kinetic growth regime, whereas equilibrium nanocrystals with low aspect ratios were obtained in the slow growth under thermodynamic control. On the other hand, because the amino acids have a coordinating effect on the control of crystal morphology, urchin-like (Fig. 6(A)) rather than round sphere CdS crystals were formed even at low temperature of 160 °C.

We investigated the UV–vis absorption characteristics of our CdS dendritic crystals and nanoparticles to demonstrate the influence of crystal shapes on the optical properties (Fig. 8). Fig. 8(A) illustrates, from curve 1 to curve 6, the absorption spectra obtained from the CdS crystals shown in 2(A), 3(C) and (E), 4(C), 7(D) and (E), respectively. Although broad scattering bands covering a wide range from visible light to the near-infrared region due to the large size of the crystals appeared in the absorption spectrum, the intrinsic band gap absorption of the samples remained in the 400–600 nm range. Interestingly, the dendrites consisting of a main trunk and rod-like branches have absorption peaks at 533 nm (curve 1 and curve 3 in Fig. 8(A)), while the peaks are shifted to ~508 nm for the flower-like CdS crystals. Furthermore, it can be seen in Fig. 8(B) that the scattering band of CdS nanoparticles is weaker and the absorption peak is blue shifted to at ~480 nm due to the reducing of crystal size. These results suggest that the varied shapes exhibit different absorption characteristics and blue-shift as compared to the absorption of the bulk CdS [48], mostly due to the quantum-size effect.

4. Conclusions

Various novel CdS dendrites were synthesized through a facile amino acid assisted hydrothermal process. We elucidated that the side group of the amino acids plays a crucial role in determining the morphology of CdS crystals. The reaction temperature, reaction time, and concentration of amino acids were also found to have great influence on the formation of CdS crystals. Furthermore, the difference in crystal morphology greatly changed the UV–vis absorption characteristics. Our results demonstrate the possibility to fine control over the morphology of CdS crystals by slightly changing the structure of amino acids and in turn tailoring their optical properties. Our hierarchical CdS crystals may be used as ideal building blocks for optoelectronic devices, in particular photocatalyzer, due to their combined features of micro-sized with nano-sized crystals.

Acknowledgements

The authors wish to thank the National Natural Science Foundation of China (Grants 50990063, 50973095, 51011130028 and 51002136) for financial support.

References

[1] D.J. Milliron, S.M. Hughes, Y. Cui, L. Manna, J. Li, L.W. Wang, A.P. Alivisatos, Nature 430 (2004) 190.
[2] I. Patla, S. Acharya, L. Zeiri, J. Israilachvili, S. Efrima, Y. Golan, Nano Lett. 7 (2007) 1459.
[3] J.H. Peng, Y.H. Xu, H. Wu, M. Hojamberdiev, Y.H. Fu, J. Wang, G.Q. Zhu, J. Alloys Compd. 490 (2010) L20.
[4] Q.L. Huang, H. Chen, Y.C. Zhang, C.L. Wu, J. Alloys Compd. 509 (2011) 6382.
[5] J. Zhou, G.L. Zhao, J.J. Yang, G.R. Han, J. Alloys Compd. 509 (2011) 6731.
[6] V. Pardo-Yissar, E. Katz, J. Wasserman, I. Willner, J. Am. Chem. Soc. 125 (2003) 622.
[7] Y.C. Zhang, G.Y. Wang, X.Y. Hu, J. Alloys Compd. 437 (2007) 47.
[8] B. Ding, M.M. Shi, F. Chen, R.J. Zhou, M. Deng, M. Wang, H.Z. Chen, J. Cryst. Growth 311 (2009) 1533.
[9] S.L. Zhong, L.F. Zhang, Z.Z. Huang, S.P. Wang, Appl. Surf. Sci. 257 (2011) 2599.
[10] F. Lu, W. Cai, Y. Zhang, Adv. Funct. Mater. 18 (2008) 1047.
[11] S. Cho, K.H. Lee, Cryst. Growth Des. 10 (2010) 1289.
[12] J.K. Dongre, M. Ramrakhiani, J. Alloys Compd. 487 (2009) 653.
[13] X.X. Ren, G.L. Zhao, H. Li, W. Wu, G.R. Han, J. Alloys Compd. 465 (2008) 534.
[14] A.A. Yadav, E.U. Masumdar, J. Alloys Compd. 509 (2011) 5394.
[15] P. Chawla, S.P. Lochab, N. Singh, J. Alloys Compd. 509 (2011) 72.
[16] Y.Z. Fan, M.H. Deng, G.P. Chen, Q.X. Zhang, Y.H. Luo, D.M. Li, Q.B. Meng, J. Alloys Compd. 509 (2011) 1477.
[17] S.L. Xiong, B.J. Xi, C.M. Wang, G.F. Zou, L.F. Fei, W.Z. Wang, Y.T. Qian, Chem. Eur. J. 13 (2007) 3076.
[18] D.J. Wang, D.S. Li, L. Guo, F. Fu, Z.P. Zhang, Q.T. Wei, J. Phys. Chem. C 113 (2009) 5984.
[19] Y. Guo, H. Zhang, Y. Wang, Z.L. Liao, G.D. Li, J.S. Chen, J. Phys. Chem. B 109 (2005) 21602.
[20] Q. Wang, G. Chen, C. Zhou, R.C. Jin, L. Wang, J. Alloys Compd. 503 (2010) 485.
[21] F. Chen, R.J. Zhou, L.G. Yang, N. Liu, M. Wang, H.Z. Chen, J. Phys. Chem. C 112 (2008) 1001.
[22] Q.Q. Wang, G. Xu, G.R. Han, Cryst. Growth Des. 6 (2006) 1776.
[23] F. Lia, W.T. Bi, T. Kong, C.J. Wang, Z. Li, X.T. Huang, J. Alloys Compd. 479 (2009) 707.
[24] J.F.A. Oliveira, T.M. Milão, V.D. Araújo, M.L. Moreira, E. Longo, M.I.B. Bernardi, J. Alloys Compd. 509 (2011) 6880.
[25] D.S. Dhawale, D.P. Dubal, R.J. Deokate, T.P. Gujar, Y.K. Sun, C.D. Lokhande, J. Alloys Compd. 503 (2010) 422.
[26] D. Mo, J. Liu, H.J. Yao, J.L. Duan, M.D. Hou, Y.M. Sun, Y.F. Chen, Z.H. Xue, L. Zhang, J. Cryst. Growth 310 (2008) 612.
[27] M. Lei, L.Q. Qian, Q.R. Hu, S.L. Wang, W.H. Tang, J. Alloys Compd. 487 (2009) 568.
[28] T. Shanmugapriya, R. Vinayakan, K.G. Thomas, P. Ramamurthy, Cryst. Eng. Commun. 13 (2011) 2340.
[29] Z.G. Cheng, S.Z. Wang, D.J. Si, B.Y. Geng, J. Alloys Compd. 492 (2010) L44.
[30] Z.P. Zhang, X.Q. Shao, H.D. Yu, Y.B. Wang, M.Y. Han, Chem. Mater. 12 (2005) 332.
[31] K.F. Li, Q.J. Wang, X.Y. Cheng, T.X. Lv, T.K. Ying, J. Alloys Compd. 504 (2010) L31.
[32] M.H. Chen, Y.N. Kim, C.C. Li, S.O. Cho, Cryst. Growth Des. 8 (2008) 629.
[33] F. Gao, Q.Y. Lu, X.K. Meng, S. Komarneni, J. Phys. Chem. C 112 (2008) 13359.
[34] Q.Y. Lu, F. Gao, S. Komarneni, J. Am. Chem. Soc. 126 (2004) 54.
[35] M. Valodkar, A. Pal, S. Thakore, J. Alloys Compd. 509 (2011) 523.
[36] F. Chen, R.J. Zhou, L.G. Yang, M.M. Shi, G. Wu, M. Wang, H.Z. Chen, J. Phys. Chem. C 112 (2008) 13457.
[37] L. Liu, L. Fu, Y. Liu, Y.L. Liu, P. Jiang, S.Q. Liu, M.Y. Gao, Z.Y. Tang, Cryst. Growth Des. 9 (2009) 4793.
[38] L.Y. Chen, Z.D. Zhang, W.Z. Wang, J. Phys. Chem. C 112 (2008) 4117.
[39] F. Zuo, S. Yan, B. Zhang, Y. Zhao, Y. Xie, J. Phys. Chem. C 112 (2008) 2831.
[40] J.H. Jiang, R.L. Yua, R. Yi, W.Q. Qin, G.Z. Qiu, X.H. Liu, J. Alloys Compd. 493 (2010) 529.
[41] J. Pan, S.L. Xiong, B.J. Xi, J.G. Li, J.Y. Li, H.Y. Zhou, Y.T. Qian, Eur. J. Inorg. Chem. 35 (2009) 5302.
[42] J.H. Xiang, H.Q. Cao, Q.Z. Wu, S.C. Zhang, X.R. Zhang, A.R. Andrew, J. Phys. Chem. C 112 (2008) 3580.
[43] S.L. Xiong, B.J. Xi, C.G. Wang, D.C. Xu, X.M. Feng, Z.C. Zhu, Y.T. Qian, Adv. Funct. Mater. 17 (2007) 2728.
[44] X.Y. Chen, X. Wang, Z.H. Wang, X.G. Yang, Y.T. Qian, Cryst. Growth Des. 5 (2005) 347.
[45] X.B. He, L. Gao, J. Phys. Chem. C 113 (2009) 10981.
[46] Y.J. Xiong, Y. Xie, J. Yang, R. Zhang, C.Z. Wu, G.A. Du, J. Mater. Chem. 12 (2002) 3712.
[47] C.J. Murphy, N.R. Jana, Adv. Mater. 14 (2002) 80.
[48] S.W. Chae, H.W. Shin, E.S. Lee, E.J. Shin, J.S. Jung, Y.R. Kim, J. Phys. Chem. B 109 (2005) 6204.
[49] K. Yamaguchi, T. Yoshida, T. Sugiura, H. Minoura, J. Phys. Chem. B 102 (1998) 9677.
[50] Y.D. Yin, A.P. Alivisatos, Nature 437 (2005) 664.